The H + D_2 → HD + D Reaction. Quasiclassical Trajectory Study of Cross Sections, Rate Constants, and Kinetic Isotope Effect

F. J. Aoiz,[†] L. Bañares,[†] V. J. Herrero,*[,‡] V. Sáez Rábanos,[§] and I. Tanarro[‡]

Departamento de Química Física, Facultad de Química, Universidad Complutense, 28040 Madrid, Spain, and Instituto de Estructura de la Materia (CSIC), Serrano 123, 28006 Madrid, Spain, and Departamento de Química General y Bioquímica, ETS Ingenieros de Montes, Universidad Politécnica, 28040 Madrid, Spain

Received: April 21, 1997; In Final Form: June 6, 1997[⊗]

The quasiclassical trajectory method has been applied to the calculation of cross sections and rate constants for the H + D_2 → HD +D reaction on three *ab initio* potential energy surfaces. The results include state-selected cross sections for the reaction with D_2(v=0,j=0−9) and D_2(v=1,j=0) and thermal rate constants in the 200−1500 K temperature range. A global good agreement is found between the present results and those from experiment and from approximate quantum mechanical calculations. This agreement is particularly good between 200 and 900 K. At higher temperatures, the quasiclassical rate constants deviate gradually toward lower values. A detailed comparison is performed between the reactivity of this isotopic variant and that of D + H_2. Special attention is paid to the effect of rotational excitation on reactivity, which is opposite for the two isotopomers, and to the microscopic dynamics responsible for the observed ratio of thermal rate constants and cross sections. In particular, the larger reaction cross section of D + H_2 as compared with H + D_2 is found to be caused by the more efficient transfer of collision energy from the heavier D atom to the molecular bond of the lighter H_2 molecule. These findings can be rationalized with simple dynamical models.

I. Introduction

The difference in the thermal rate constants *k(T)* for the D + H_2 and H + D_2 reactions is a paradigmatic example of the kinetic isotope effect (KIE).[1] Since the early experimental data on the kinetics of the H_3 system were reported,[2] the smaller reactivity of the H + D_2 isotopic variant was traced back to its higher activation energy, which was in turn attributed to the smaller zero-point energy of D_2 as compared with H_2. The conventional transition state theory (TST) of reaction rates[1] could account satisfactorily for the observed rate constant ratio, but the absolute values of the rate constants predicted by the classical TST were much too low and refinements including tunneling corrections had to be introduced in order to achieve agreement with experiment (see refs 2−4 and references therein). A rigorous dynamic approach to the calculation of rate constants has required a much more considerable effort (see refs 5−7 and references therein), and a detailed comparative study of the rates of the isotopic variants of H_3 from a dynamic point of view is, in many aspects, still lacking.

In recent times, accurate quantum mechanical (QM) calculations of thermal rate constants *k(T)*[5,6,8] performed on three *ab initio* potential energy surfaces (PESs)[9−11] have been reported for the D + H_2 isotopic variant of the reaction. The three *ab initio* surfaces used are, at first sight, very similar, and detailed QM sensitivity analyses[12−15] have been dedicated to the investigation of the subtle differences in reactivity associated with the peculiarities of each PES and of the various isotopomers of H_3. In this respect, it is interesting to observe how the calculation of such a "bulk" quantity as the thermal rate constant can provide both a link to experiment and a sensitive way of discriminating between similar PESs. The accurate QM calculations of Mielke et al.[6] for D + H_2 showed appreciable differences between the results obtained on the surface of Boothroyd et al.[11] (hereafter BKMP) and those obtained on the surfaces of Liu−Siegbahn−Truhlar−Horowitz[9] and of Varandas et al.[10] (hereafter, LSTH and DMBE, respectively). The agreement between the QM results and the available experimental data (see refs 3, 16−19 and references therein) is good, although the rate constants calculated on the BKMP PES are somewhat larger than the experimental ones for temperatures below 800 K (up to a factor of 2 at 200 K). In the temperature region beyond 1000 K all the rate constants obtained with accurate QM methods deviate gradually from the measurements so that at 1500 K the calculated values are 30−50% lower than the experimental ones. The determination of a bulk quantity, such as rate constants, directly comparable to experiment, from the solution of the microscopic equations of motion has demonstrated the impressive progress of the theoretical methodology in the field of reaction dynamics during the last decade, but has also shown that, at present, the computational complications inherent to these accurate methods limit decisively their general applicability and make problematic their extension to larger systems and higher energies.

The exploration of approximate theoretical approaches of sufficient accuracy but computationally simpler is thus very attractive, and the experiments and accurate calculations for D + H_2 mentioned in the previous paragraph provide an ideal standard for other theoretical methods. Several QM methods based on the *J*-shifting approximation[5,6,19−21] have been successfully applied to the calculation of rate constants for this reaction. Another possible approach is the use of the quasiclassical trajectory (QCT) method, as in a previous work[7] from our group where calculations of cross sections and rate constants for the D + H_2(v=0,1) reaction were carried out on the three *ab initio* PESs.[9−11] A fairly good agreement with QM and experiment was obtained. For a given temperature the thermal rate constants showed the same relative dependence on the PES as the quantum mechanical ones. The QCT study provided a rationale for this fact in terms of the (slightly) distinct topological

* Corresponding author.
[†] Universidad Complutense.
[‡] Instituto de Estructura de la Materia.
[§] Universidad Politécnica.
[⊗] Abstract published in *Advance ACS Abstracts,* August 1, 1997.

S1089-5639(97)01368-6 CCC: $14.00 © 1997 American Chemical Society

properties of the PESs. The agreement between QM and QCT is particularly good for the reaction of the atoms with rotationless hydrogen molecules, but the QCT thermal rate constants are smaller than their experimental and quantum mechanical counterparts, the differences being caused by the increase in the classical threshold with growing rotational quantum number, j, of the H_2 molecule.[7]

This increase in the classical threshold was already recognized in the pioneering QCT calculations of Karplus et al.[22a] for the $H + H_2$ reaction performed on the relatively precise empirical PES of Porter and Karplus.[22b] These authors interpreted this fact as due to the decrease in the beneficial orienting effect of the PES (tending to steer the reagents toward a collinear configuration) with growing rotation of the hydrogen molecule. Since the work of Karplus et al.[22] a great number of trajectory calculations and simple models have dealt explicitly with the influence of rotation on reactivity in atom−diatom systems (see refs 23−43 and references cited therein). All these treatments share the central idea that most of the observed effects of rotational excitation on reactivity are related to the dynamic reorientation caused by the anisotropy of the potential in the course of a reactive collision. These effects depend on the shape of the PES as well as on the collision energy and on the rotational state of the reacting molecule and are more pronounced for collision energies close to threshold and for the lower rotational levels. All the realistic PESs for the reactive $H + H_2$ system, and in particular the *ab initio* ones, present a barrier to reaction which is lowest in the collinear configuration. The usual behavior found for this type of surface at low collision energies is an initial decrease of the reaction cross section with growing rotational excitation, followed by a minimum and a subsequent rise for high enough values of j. This behavior was indeed obtained in different QCT calculations for the $H + H_2$[25,27] and $D + H_2$[7,30,44] isotopic variants. Although accurate QM studies of the effect of rotation are much more limited than those from QCT, there are some results available for $D + H_2$.[5,45] The existing data for $D + H_2(v=1)$[5] indicate also a negative influence of rotation on reactivity in the post threshold region. However, in the classical case the effect is enhanced in the vicinity of the barrier to reaction[7] and results in an upward shifting of the threshold with increasing j. In the QM calculation,[5] a decrease of the cross section with growing j is also observed, but practically the same threshold is obtained for all the rotational states of the molecule.

The dynamical features underlying the observed macroscopic rate of the $H + D_2$ isotopic variant have not been so thoroughly investigated. Many experimental studies have indeed been devoted to the microscopic dynamics of $H + D_2$. The experimental data include total[46−49] and differential[50−58] cross sections as well as distributions of internal states of the nascent products.[49,50,53,54,56−61] Theoretical calculations using accurate QM methods,[63−67] quantum mechanical approximations,[68−74] and quasiclassical trajectories[53,54,56,57,75−80] have also been performed for the conditions of the measurements, and in most cases a good agreement was found between theory and experiment. In particular, the highest resolution state resolved differential cross sections, and the most precise comparisons between theory and experiment available for the $H + H_2$ system have been reported for this isotopic variant.[54] However, the dynamical experiments just mentioned have been usually performed with "hot" H atoms generated by photolysis and sample regions of comparatively high energy in the potential surface that are of little relevance to the measured rate constants. The most valuable information about the reactivity at threshold still comes from rate constant data. The $H + D_2$ rate constant measurements of the 1960s[3,81] have been extended more recently both in the high-[19,82] and low-temperature[83] regimes. At present, the data available on thermal rate constants span the temperature range from 274 to 2061 K. Reduced dimensionality QM calculations of rate constants[19,84] performed on the DMBE PES are in good agreement with the measurements over the whole temperature range, but, as far as we know, no accurate QM calculations or detailed studies of the dynamics on the various *ab initio* PES comparable to those of $D + H_2$[6,7] have been reported.

Due to the relatively high classical barrier for the H_3 reactive system, "threshold effects" are very important for the macroscopic reaction rate over a wide temperature range; even at 2000 K the average collision energy is ∼0.26 eV, still below the classical threshold for reaction. This preponderance of threshold effects and the fact commented on above, that the different zero-point energies of the molecules of hydrogen and deuterium lead to distinct thresholds for the $D + H_2$ and $H + D_2$ reactions, has provided since the very beginning a satisfactory explanation based on purely energetic grounds for the large differences found in the rate constants of the two isotopic variants, especially at low temperatures. The early success in the explanation of the rate constant ratio has masked for a long time other interesting dynamical differences between the two isotopomers. The existing cross section data for the hydrogen exchange reaction indicate not only a higher threshold but also a significantly slower growth of the excitation function, $\sigma_R(E_T)$ (*i.e.* the collision energy dependence of the reaction cross section), for $H + D_2$[47,49,74,75,79] as compared to that for $D + H_2$.[74,75,85,86] A similar isotopic behavior has been found recently in cross section measurements for the $D^- + H_2 \rightarrow HD + H^-$ and $H^- + D_2 \rightarrow HD + D^-$ ion−molecule reactions.[87] The dynamical implications of this different behavior are not yet totally clear. Song and Gislason[88] have applied their "pairwise energy model" (PEM) in order to justify the relative reaction cross sections obtained in QCT calculations for various isotopomers of H_3. This model assumes that the relative reaction cross sections of the different isotopic variants of an $A + BC \rightarrow AB + C$ reaction is dependent only on the initial kinetic energy of the AB pair. The model works well at very high energies (typically several electronvolts) but breaks down for lower collision energies, like those relevant for the measured rate constants, due to limitations that are discussed by the authors.

For the conditions of the kinetic experiments, diverse dynamical factors could be of importance for the isotope effect. In the crucial post-threshold region, the possible orienting influence of the surface could be felt in a different way by the various isotopomers of a chemical reaction due to their distinct kinematics. In addition, the effects of rotation might also depend on the particular isotopic variant, since for the same PES and for a given collision energy and rotational state of the molecule, the ratio of the atom−diatom radial velocity to the angular velocity of the diatom is very different, and this difference could have an observable influence on the thermal rate constants, especially at low temperatures. On the other hand, the efficiency of transfer of the collision energy to the molecular bond to be broken should not be the same for all the isotopic variants due to the different combinations of atomic masses involved, and this could also contribute to the distinct isotopic reactivity.

In an attempt to clarify these questions and to check further the validity of the QCT method for the calculation of rate constants, we extend here our previous investigation of the kinetics of $D + H_2$ to the $H + D_2$ isotopic variant of the reaction. For the present work, we have calculated excitation functions for individual rotational states $j = 0−9$ of the $D_2(v=0)$ molecule

and $j = 0$ of the $D_2(v=1)$ molecule on the three *ab initio* PESs. In addition, we have calculated excitation functions for the H + $D_2(v=1)$ reaction averaged on initial j for temperatures in the range 800−1500 K. These state-selected and averaged excitation functions have been used to calculate thermal rate constants in the 200-1500 K temperature range. The results are discussed, analyzed in terms of simple intuitive models, and, when available, compared to other theoretical data and to experiment.

II. Method

The general method for the calculation of quasiclassical trajectories used in the present work is similar to the one described previously (see, for instance, refs 44, 86). As in previous publications,[7,43,89,90] the determination of the collision energy (E_T) dependence of the reaction cross section, $\sigma_R(E_T)$, is done by running batches of trajectories where the collision energy is sampled randomly within the interval $[E_1,E_2]$ in addition to the rest of initial conditions. Since in the present calculations the number of initial states of the reactants to be considered and the collision energy interval are quite large, the computational efficiency of the QCT methodology is markedly improved by using this procedure in comparison to the traditional method of running batches of trajectories at fixed collision energy.

The E_1 energy value is chosen so that the collisional threshold, E_0, is larger than E_1; the E_2 energy value is chosen to be 1.6 eV, in order to determine rate constants *k(T)* up to 1500 K. Once the value of the collision energy is randomly (uniformly) sampled within $\Delta E = E_2 - E_1$, the impact parameter b is obtained for every trajectory as

$$b = \beta^{1/2} b_{max}(E_T) \tag{1}$$

where β is a random number in the [0,1] interval, and the maximum impact parameter, b_{max}, at a given collision energy, E_T, is given by

$$b_{max}(E_T) = D\left(1 - \frac{E_D}{E_T}\right)^{1/2} \tag{2}$$

The values of the parameters D and $E_D < E_1 < E_0$ are previously determined by fitting the values of the maximum impact parameters, found at several selected collision energies, E_T, to the line-of-the-centers expression of eq 2. The resulting $b_{max}(E_T)$, as given by eq 2, are such that, for the selected E_T, there are no reactive trajectories for impact parameters larger than b_{max}. With this kind of energy dependent sampling of the impact parameter, each trajectory is weighted by $w_i = b_{max}^2/D^2$.

The integration step size in the trajectories was chosen to be 5×10^{-17} s. This guarantees a conservation of the total energy better than 1 in 10^5 and better than 1 in 10^7 in the total angular momentum. The initial rovibrational energies of the D_2 molecule in $v = 0$ and 1 are calculated using a Dunham expansion containing 16 terms[91−93] (fifth power in $v + 1/2$ and third power in $j(j + 1)$). The classical D_2 molecule rotational angular momentum is equated to $j(j + 1)\hbar^2$.

Batches of 120 000 trajectories for every v,j rovibrational state of D_2 have been run in the energy range $[E_1,E_2]$ on each of the three *ab initio* PESs (LSTH, DMBE, and BKMP). For the lowest initial rotational states of $D_2(v=0,j=0-4)$, the stratified sampling technique[94] was used to decrease the statistical uncertainty near the threshold. To this purpose, extra batches of 120 000 trajectories were run for $D_2(v=0,j=0-4)$ in a restricted range of collision energies with E_2 not higher than 0.6 eV. The whole set of trajectories was then weighted accordingly. In addition, batches of 150 000 trajectories were run for the H + $D_2(v=1,j=0)$ reaction on the three PESs.

As in previous work,[7,43,89,90] $\sigma_R(E_T)$ was subsequently calculated by the method of moments expansion in Legendre polynomials (see refs 86 and 94) using the reduced variable

$$x = \frac{2E_T - E_2 - E_1}{\Delta E} \tag{3}$$

where $\Delta E = E_2 - E_1$. The expression for $\sigma_R(E_T)$, truncated in the Mth term, is given by

$$\sigma_R(E_T) = \frac{2R}{\Delta E}\left[\frac{1}{2} + \sum_{n=1}^{M} c_n P_n(x)\right] \tag{4}$$

where R is the Monte Carlo estimate of the integral

$$R = \langle \sigma_R(E_T) \rangle \Delta E = \int_{E_1}^{E_2} \sigma_R(E_T) dE_T \approx \pi D^2 \Delta E \frac{S_{N_R}}{N} \tag{5}$$

where N is the total (reactive and nonreactive) number of trajectories, and the sum of the weights of the reactive trajectories (w_i), S_{N_R}, is given by

$$S_{N_R} = \sum_{i=1}^{N_R} w_i \tag{6}$$

The coefficients of the Legendre expansion, c_n, of eq 4 are calculated as the Monte Carlo average of Legendre moments:

$$c_n = \frac{2n+1}{2} \frac{1}{S_{N_R}} \sum_{i=1}^{N_R} w_i P_n(x_i) = \frac{2n+1}{2} \langle P_n \rangle \tag{7}$$

In order to calculate the errors in the reaction cross sections, thresholds, and rate constants, an estimate of the error of the coefficients is needed and can be easily found as

$$\gamma_n^2 \equiv \mathrm{var}[c_n] = S_{N_R}^{-1}\left[\left(\frac{2n+1}{2}\right)^2 \langle P_n^2 \rangle - c_n^2\right] \tag{8}$$

The error in $\sigma_R(E_T)$ is given by the square root of the variance, which can be evaluated in terms of γ_n as

$$\mathrm{var}[\sigma_R(E_T)] = \frac{N - S_{N_R}}{N S_{N_R}} [\sigma_R(E_T)]^2 + \left(\frac{2R}{\Delta E}\right)^2 \sum_{n=1}^{M} \gamma_n^2 P_n^2(x) \tag{9}$$

The Smirnov−Kolmogorov test comparing the cumulative probability distributions was used to decide when to truncate the series of eq 4. Significance levels higher than 98% could be achieved using 6−10 Legendre moments, ensuring good convergence such that the inclusion of more terms does not produce any significant change. The translational energy threshold, E_0, for every initial rovibrational state is determined by finding the roots of eq 4 by the Newton−Raphson method. Special care was paid to the analysis of the threshold in the $\sigma_R(E_T)$, which remains unaffected, within the statistical uncertainty, when the number of Legendre moments are changed by ±2. The error bars correspond to plus/minus one standard deviation, calculated according to eq 9.

The specific thermal rate constant from the v,j initial state of the D_2 molecule is given by

$$k_{v,j}(T) = \left(\frac{8k_BT}{\pi\mu_{D,H_2}}\right)^{1/2} (k_BT)^{-2} \int_0^\infty \sigma_R(E_T;v,j) E_T \exp\left(\frac{-E_T}{k_BT}\right) dE_T \quad (10)$$

where μ is the reduced mass of the H,D_2 system, k_B is the Boltzmann constant, and $\sigma_R(E_T;v,j)$ represents the translational excitation function for the H + $D_2(v,j)$ reaction. In practice, the lower limit in the integral is E_0 and the upper limit is E_2.

The thermal (averaged on initial j) rate constant from an initial vibrational state can be written as

$$k_v(T) = \sum_{j=0}^{9} p_{v,j}(T) k_{v,j}(T) \quad (11)$$

where $p_{v,j}(T)$ are the Boltzmann's statistical weights of the D_2 rotational states (including the 2:1 nuclear spin weights), such that $\sum_j p_{v,j}(T) = 1$. At $T = 700$ K, the $v = 0$ population is 99.5%, whereas at 1500 K it is 87.23%. Therefore, the contribution from $v = 1$ cannot be neglected at $T > 800$K. To obtain thermal rate constants for the H + $D_2(v=1)$ reaction, instead of running trajectories for each individual initial j state, it was preferred to calculate thermally averaged excitation functions for $v = 1$ using the same method as described above, but, additionally, sampling randomly the initial j state from the Boltzmann distribution at each temperature. Unless otherwise specified, the reactions with thermal H_2 and D_2 refer to normal n-H_2 (25% para, 75% ortho) and n-D_2 (66.6% ortho, 33.3% para). From these results, $k(T,v=1)$ are calculated via eq 10, and the final thermal $k(T)$ are calculated by taking into account the relative populations in $v = 0$ and $v = 1$ at each temperature. The estimation of the errors of the rate constants was performed as in ref 7.

III. Results and Discussion

III.1. Cross Sections and Rate Constants. The excitation functions calculated for the H + $D_2(v=0;j=0,3,5,7,9)$ reaction on the LSTH PES[9] are shown in the top panel of Figure 1, and those on the DMBE[10] and BKMP[11] PESs are shown in the top panels of Figures 2 and 3, respectively. In all cases, the cross section grows monotonically from threshold until they stabilize at a collision energy close to 1.2 eV. Rotational excitation is seen to have always a beneficial influence on reactivity; the threshold for reaction shifts slightly to lower energies and the value of the cross section grows with increasing j. The reaction thresholds for rotationless molecules are coincident on the three PESs considered, and the excitation functions on the DMBE and BKMP PESs are nearly identical and slightly larger than that on the LSTH. The increase in cross section with rotational excitation is smaller on the DMBE PES than on the other two, especially in the immediate post threshold region (see insets in top panels of Figures 1−3).

It is most interesting to observe the contrasting behavior obtained for the reaction cross sections of the two isotopomers. The results for D + H_2[7] are shown in the lower panels of Figures 1−3. For the three potential surfaces, the thresholds are smaller, the cross sections larger, and, most notably , the effect of rotational excitation at low collision energy is opposite, *i.e.* negative for D + H_2 and positive for H + D_2. QCT calculations on the LSTH surface are also available for H + H_2.[25,27] In the latter case, the situation with respect to rotational excitation is intermediate: the net effect of rotation is negative but very slight. As expected, the present QCT results are in good accordance with the various QCT calculations previously reported[75−79] for H + D_2 on the LSTH and DMBE PESs for initial conditions within the range considered in this work. Cross section values from accurate QM calculations have been reported

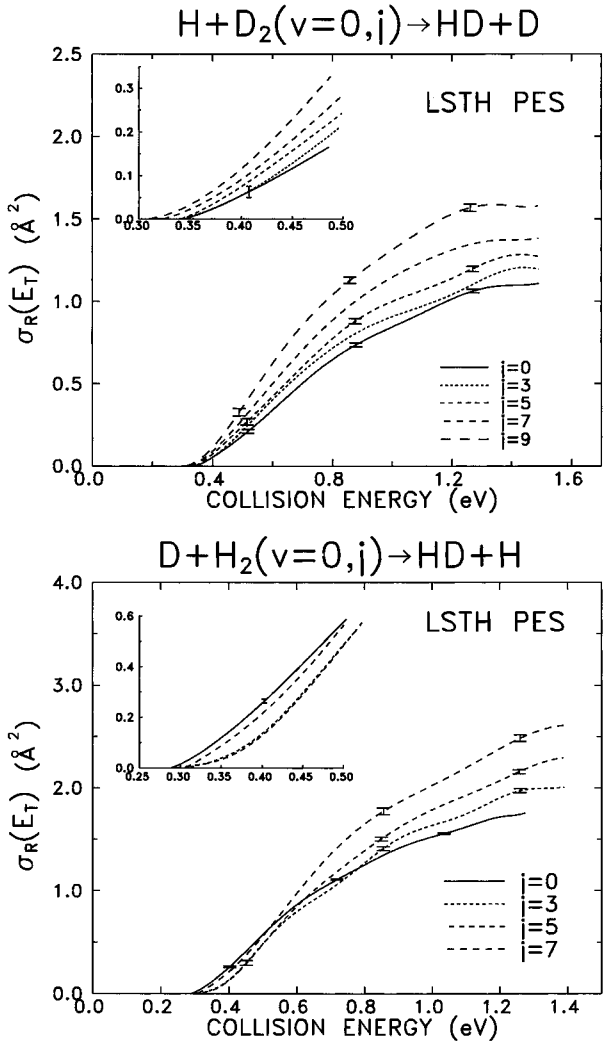

Figure 1. Present QCT reaction cross sections as a function of collision energy (excitation function) for the H + $D_2(v=0,j)$ → HD + D (top panel) and D + $H_2(v=0,j)$ → HD + H (bottom panel) reactions at the indicated initial rotational quantum number j calculated on the LSTH PES. The insets display the cross sections near the reactive threshold. The error bars indicate one standard deviation of the calculations.

for H + $D_2(v=0,j=0-2)$ by two different groups[63,64] at ∼0.54 eV collision energy on the LSTH and BKMP PESs and at 1.30 eV on the LSTH surface.[63] The agreement with the present results is very good, as shown in Table 1. There is also good accordance with the various experimental determinations of absolute reaction cross sections within the collision energy range studied here.[46−49] No systematic measurements of the D + H_2/H + D_2 cross section ratio have been reported in the literature, but, interestingly, the recent experimental determination of the cross sections of the D^- + H_2 → HD + H^- and H^- + D_2 → HD + D^- ion molecule reactions reveals an isotopic behavior very similar to the one described here.[87]

Figure 4 shows the excitation functions calculated for the D + $H_2(v=1,j=0)$ and H + $D_2(v=1,j=0)$ reactions on the BKMP PES. For the two reactions, the threshold decreases appreciably and the cross sections become larger with vibrational excitation. In any case, the difference of reactivity between the two isotopic variants persists. The results on the other two PESs (not shown) are similar to those presented here.

The excitation functions of Figures 1−4 have been used to calculate state specific rate constants for the H + $D_2(v=0,1;j=0)$ reactions in the 200−1500 K temperature range. The results are listed in Tables 2 and 3. For each initial vibrational state, the rate constants on the three PESs are very similar and lie all

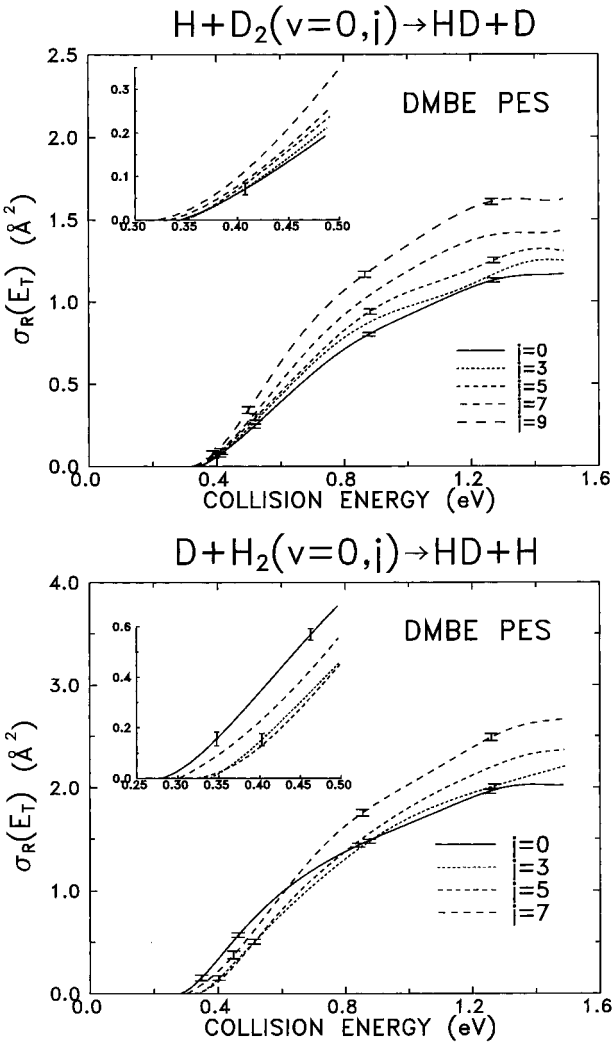

Figure 2. Same as Figure 1 but for the DMBE PES.

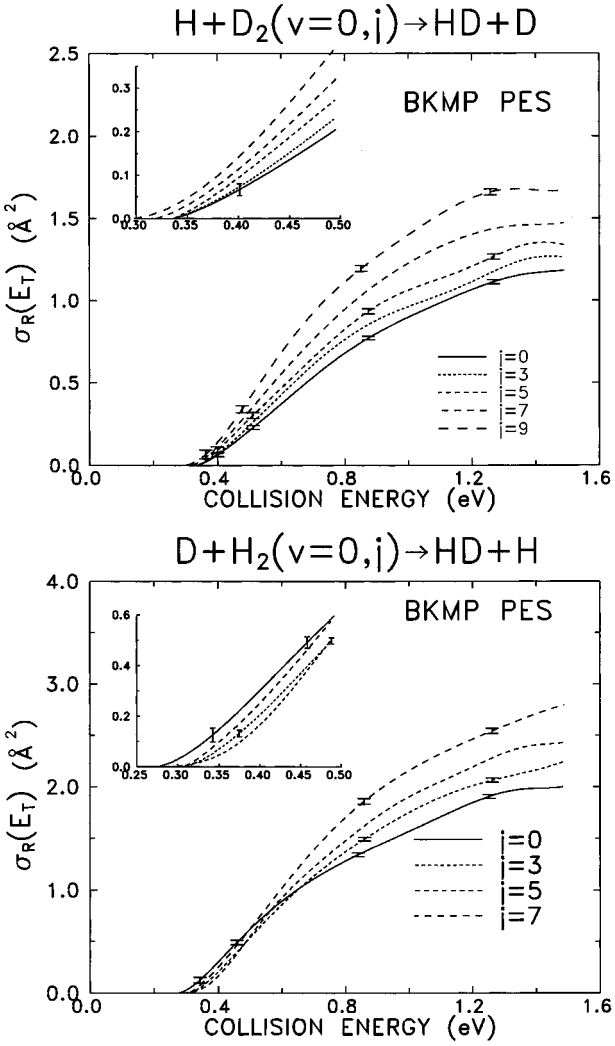

Figure 3. Same as Figure 1 but for the BKMP PES.

within the mutual statistical uncertainty up to 800 K. For higher temperatures, the $j = 0$ rate constants for the DMBE and BKMP PESs are nearly identical and slightly larger than those on the LSTH PES.

Thermal rate constants were calculated on the three surfaces between 200 and 1500 K using the specific rate constants for the H + $D_2(v=0,j=0-9)$ reactions. For temperatures larger than 800 K, the contribution from the H + $D_2(v=1)$ reaction has to be taken into account, as indicated in the Method section. The QCT thermal rate constants on the three surfaces bear a great similarity, and their values overlap up to 800 K within the statistical uncertainties. From Tables 2−4 and from the thermal populations of molecular levels, one can see that rotational excitation leads to an increase in the rate constants on the LSTH and BKMP surfaces that begins to be appreciable from ∼500 to 600 K; the effect of rotation is much smaller on the DMBE PES over the whole temperature range studied. For temperatures higher than ∼800 K the contribution of the first vibrational state rate begins also to be important (the $v = 1$ population is always small, but the reaction with $D_2(v=1)$ has a much smaller threshold), and in fact, at 1500 K the contribution of the first vibrational state accounts for ∼17% of the rate constant value. At the same temperature, the rate constant for reaction with $D_2(v=0,1;j=0)$ is about 10% smaller than that for reaction with $D_2(v=0,1;$thermal $j)$ on the LSTH and BKMP surfaces, whereas it is only 2% smaller in the case of the DMBE PES.

In Table 4 and in Figures 5 and 6, the QCT thermal rate constants on the three PESs are compared to the experimental measurements[3,19,81−83] and to the results of reduced dimensionality QM calculations on the DMBE surface.[19] In particular, the values labeled as "experimental" in Table 4 and in Figure 6 correspond to the three-parameter fit to most experimental data provided in ref 82. As can be seen, the accord of the present results with the majority of the experimental measurements and with the approximate QM results is very good in the 200−800 K temperature range. Although the three PESs perform well, the best global agreement is obtained on the

TABLE 1: QM and QCT Integral Reaction Cross Sections σ_R (Å^2) for the H + $D_2(v=0,j)$ → HD + D Reaction Calculated on the LSTH and BKMP PESs at the Indicated Collision Energies, E_T, and Initial Rotational Quantum Number, j

E_T (eV)	j	PES	QM[a]	QCT[c]
0.546 36	0	LSTH	0.277	0.257 ± 0.011
0.550 00	0	LSTH	0.282 (0.284[b])	0.261 ± 0.011
0.539 94	1	LSTH	0.274	0.267 ± 0.011
0.525 15	2	LSTH	0.260	0.249 ± 0.012
0.540 00	0	BKMP	0.292	0.275 ± 0.012
0.547 41	0	BKMP	0.306	0.287 ± 0.012
0.562 20	0	BKMP	0.335	0.311 ± 0.012
0.540 00	1	BKMP	0.301	0.292 ± 0.012
0.554 79	1	BKMP	0.329	0.318 ± 0.012
0.525 21	2	BKMP	0.287	0.276 ± 0.012
0.540 00	2	BKMP	0.314	0.303 ± 0.012
1.300 00	0	LSTH	1.059[b]	1.077 ± 0.013

[a] Reference 64. [b] Reference 63. [c] Present work.

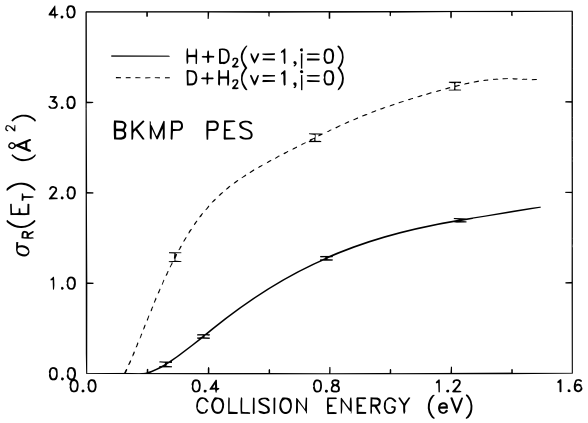

Figure 4. Excitation functions for the D + H_2(v=1,j=0) (dashed line) and H + D_2(v=1,j=0) (solid line) calculated on the BKMP PES. Error bars as in Figure 1.

TABLE 2: QCT Specific Rate Constants $k(T;j)$ (cm^3 s^{-1}) for the H + D_2(v=0,j=0) → HD + D Reaction as a Function of Temperature Calculated on the LSTH, DMBE, and BKMP PESs: Numbers in Parentheses Represent Powers of Ten

T (K)	LSTH	DMBE	BKMP
200	0.16 ± 0.10(−19)	0.18 ± 0.10(−19)	0.24 ± 0.15(−19)
250	1.03 ± 0.43(−18)	1.15 ± 0.44(−18)	1.44 ± 0.61(−18)
300	1.63 ± 0.51(−17)	1.92 ± 0.52(−17)	2.28 ± 0.69(−17)
350	1.31 ± 0.30(−16)	1.47 ± 0.31(−16)	1.69 ± 0.39(−16)
400	0.61 ± 0.11(−15)	0.69 ± 0.11(−15)	0.77 ± 0.14(−15)
450	2.06 ± 0.30(−15)	2.33 ± 0.31(−15)	2.55 ± 0.37(−15)
500	5.50 ± 0.67(−15)	6.24 ± 0.69(−15)	6.70 ± 0.81(−15)
550	1.24 ± 0.13(−14)	1.41 ± 0.13(−14)	1.49 ± 0.15(−14)
600	2.47 ± 0.22(−14)	2.81 ± 0.22(−14)	2.94 ± 0.25(−14)
700	7.41 ± 0.49(−14)	8.44 ± 0.50(−14)	8.68 ± 0.56(−14)
800	1.63 ± 0.09(−13)	1.96 ± 0.09(−13)	1.99 ± 0.10(−13)
900	3.38 ± 0.14(−13)	3.84 ± 0.14(−13)	3.86 ± 0.15(−13)
1000	5.85 ± 0.20(−13)	6.66 ± 0.20(−13)	6.63 ± 0.22(−13)
1100	9.27 ± 0.26(−13)	1.05 ± 0.03(−12)	1.04 ± 0.03(−12)
1200	1.37 ± 0.03(−12)	1.55 ± 0.03(−12)	1.53 ± 0.04(−12)
1300	1.92 ± 0.04(−12)	2.17 ± 0.04(−12)	2.13 ± 0.04(−12)
1400	2.58 ± 0.05(−12)	2.91 ± 0.05(−12)	2.85 ± 0.05(−12)
1500	3.34 ± 0.05(−12)	3.76 ± 0.05(−12)	3.68 ± 0.06(−12)

TABLE 3: QCT Specific Rate Constants $k(T;j)$ (cm^3 s^{-1}) for the H + D_2(v=1,j=0) → HD + D Reaction as a Function of Temperature Calculated on the LSTH, DMBE, and BKMP PESs: Numbers in Parentheses Represent Powers of Ten

T (K)	LSTH	DMBE	BKMP
200	0.57 ± 028(−16)	0.75 ± 0.35(−16)	1.01 ± 0.39(−16)
250	7.36 ± 2.68(−16)	0.91 ± 0.32(−15)	1.14 ± 0.33(−15)
300	0.42 ± 0.12(−14)	0.50 ± 0.14(−14)	0.60 ± 0.14(−14)
350	1.51 ± 0.34(−14)	1.74 ± 0.38(−14)	2.00 ± 0.38(−14)
400	4.01 ± 0.75(−14)	4.53 ± 0.81(−14)	5.10 ± 0.81(−14)
450	0.87 ± 0.14(−13)	0.96 ± 0.14(−13)	1.07 ± 0.14(−13)
500	1.65 ± 0.22(−13)	1.82 ± 0.23(−13)	1.98 ± 0.23(−13)
550	2.82 ± 0.32(−13)	3.07 ± 0.32(−13)	3.30 ± 0.32(−13)
600	4.43 ± 0.43(−13)	4.79 ± 0.43(−13)	5.10 ± 0.43(−13)
700	9.23 ± 0.69(−13)	9.86 ± 0.67(−13)	1.03 ± 0.07(−12)
800	1.63 ± 0.09(−12)	1.63 ± 0.09(−12)	1.79 ± 0.09(−12)
900	2.58 ± 0.12(−12)	2.63 ± 0.11(−12)	2.80 ± 0.11(−12)
1000	3.78 ± 0.14(−12)	3.97 ± 0.13(−12)	4.06 ± 0.13(−12)
1100	5.20 ± 0.16(−12)	5.46 ± 0.15(−12)	5.54 ± 0.15(−12)
1200	6.84 ± 0.18(−12)	7.17 ± 0.16(−12)	7.25 ± 0.17(−12)
1300	8.68 ± 0.20(−12)	9.08 ± 0.18(−12)	9.16 ± 0.18(−12)
1400	1.07 ± 0.02(−11)	1.12 ± 0.02(−11)	1.12 ± 0.02(−11)
1500	1.29 ± 0.02(−11)	1.35 ± 0.02(−11)	1.35 ± 0.02(−11)

BKMP one. At higher temperatures, the QCT rate constants become gradually smaller than those from the reduced dimensionality QM calculation and from the three-parameter fit to the experimental data. At 1500 K, the QCT data are about a factor of 0.6 of the mean experimental value (as given by the fit) and of 0.7 of the approximate quantal results. It should be stressed here that the QCT calculations for this isotopic variant can reproduce well the low-temperature experimental data, whereas this was not the case for the D + H_2 reaction, where the QCT thermal rate constants on the same three PESs were always lower than the measured ones for T < 400 K.

In the cases where QCT low-temperature rate constants are lower than those from experiment or from quantum mechanics, the neglect of tunneling inherent to the quasiclassical method is usually invoked as a cause. However, in our previous work on D + H_2,[7] it was found that classical and quantal excitation functions were very similar for reactive collisions with rotationless molecules and that the main discrepancies in the values of the thermal rate constants could be traced back to the higher thresholds obtained in the classical case with growing rotational excitation. This conclusion is reinforced by the findings of the present work. Unfortunately, no accurate QM calculations of systematic excitation functions and rate constants have been reported for H + D_2. However, the good agreement between the low-T quasiclassical $k(T)$ and those from approximate QM and experiment and the fact that for this isotopic variant rotational excitation leads to an enhancement of the cross section strongly suggest that the lower classical cross sections at threshold are restricted to the cases where rotation has a neat negative effect on reactivity.

The discrepancy at high temperature between QCT rate constants and experiment found here for H + D_2 was also obtained for the D + H_2 isotopic variant.[7] A possible cause for this discrepancy could be "excessive" recrossing of classical trajectories with increasing collision energies; however, it is worth noting that for both isotopomers all the theoretical high-temperature rate constants[6−8,19,21] are, to a greater or lesser extent, lower than the experimental ones. The high-temperature disagreement between experiment and theory might suggest, at first sight, possible inaccuracies of the PES with increasing collision energies, but this is unlikely since QM and QCT theoretical calculations are in very good agreement with experimental measurements of total and differential reaction cross sections for energies much higher than those relevant for the thermal rate constants at $T \leq$ 2000 K. In particular, a very recent molecular beam study for the H + D_2 reaction at 2.67 eV collision energy[95] (slightly above the conical intersection between the ground and first electronically excited states of the H_3) has shown that the experimental differential cross sections are describable with accuracy by QCT calculations on the ground PES, without invoking any participation of the electronically excited state. Therefore, even at these temperatures, it is very unlikely that nonadiabatic reactions may play any role that could explain the observed discrepancies between theoretical and experimental rate constants. Additional rate constant measurements for temperatures beyond 1000 K would certainly help to clarify this point.

III.2. Kinetic Isotope Effect. The ratio of experimental and theoretical thermal rate constants between the D + H_2 and H + D_2 reactions in the temperature interval 200−1500 K is shown in Figure 7. The experimental values have been obtained from refs 19 and 82, and the theoretical calculations correspond both to reduced dimensionality QM calculations[19] and to the classical results of the present work. At 250 K the experimental ratio is about 24, the QM one is more than 30, and the QCT one is 16−18 depending on the PES. With increasing temperature, the ratio gets gradually smaller, and at 1500 K both experiment and calculations yield a value of about 2. As mentioned in the Introduction, this kinetic isotope effect was well accounted for by the conventional TST, and the difference in the rate constants was essentially traced back to the difference in the zero-point

TABLE 4: QCT Thermal Rate Constants *k(T)* (cm^3 s^{-1}) for the H + *n*-D_2 → HD + D Reaction as a Function of Temperature Calculated on the LSTH, DMBE, and BKMP PESs: Numbers in Parentheses Represent Powers of Ten

T (K)	LSTH	DMBE	BKMP	QM;DMBE[a]	experiment[b]
200	0.16 ± 0.20(−19)	0.18 ± 0.15(−19)	0.25 ± 0.18(−19)	2.53(−20)	
250	1.06 ± 0.71(−18)	1.14 ± 0.54(−18)	1.52 ± 0.67(−18)		1.37(−18)
300	1.78 ± 0.77(−17)	1.92 ± 0.61(−17)	2.45 ± 0.75(−17)	1.92(−17)	2.11(−17)
350	1.38 ± 0.42(−16)	1.48 ± 0.34(−16)	1.84 ± 0.42(−16)		1.56(−16)
400	0.66 ± 0.15(−15)	0.70 ± 0.12(−15)	0.85 ± 0.15(−15)	7.09(−16)	7.29(−16)
450	2.25 ± 0.40(−15)	2.40 ± 0.34(−15)	2.85 ± 0.41(−15)		2.49(−15)
500	6.11 ± 0.87(−15)	6.49 ± 0.76(−15)	7.62 ± 0.91(−15)	6.84(−15)	6.79(−15)
550	1.40 ± 0.16(−14)	1.48 ± 0.15(−14)	1.63 ± 0.17(−14)		1.58(−14)
600	2.82 ± 0.28(−14)	2.98 ± 0.25(−14)	3.42 ± 0.30(−14)	3.28(−14)	3.23(−14)
700	8.63 ± 0.63(−14)	9.09 ± 0.57(−14)	1.03 ± 0.07(−13)	1.04(−13)	1.03(−13)
800	2.09 ± 0.11(−13)	2.19 ± 0.10(−13)	2.45 ± 0.12(−13)	2.56(−13)	2.57(−13)
900	4.17 ± 0.18(−13)	4.36 ± 0.17(−13)	4.83 ± 0.19(−13)	5.26(−13)	5.37(−13)
1000	7.33 ± 0.25(−13)	7.65 ± 0.23(−13)	8.40 ± 0.27(−13)	9.53(−13)	9.91(−13)
1100	1.17 ± 0.03(−12)	1.22 ± 0.03(−12)	1.33 ± 0.04(−12)	1.57(−12)	1.67(−12)
1200	1.74 ± 0.04(−12)	1.82 ± 0.04(−12)	1.96 ± 0.04(−12)	2.40(−12)	2.62(−12)
1300	2.45 ± 0.05(−12)	2.55 ± 0.05(−12)	2.74 ± 0.05(−12)	3.47(−12)	3.88(−12)
1400	3.30 ± 0.05(−12)	3.41 ± 0.05(−12)	3.76 ± 0.06(−12)	4.78(−12)	5.50(−12)
1500	4.27 ± 0.06(−12)	4.42 ± 0.06(−12)	4.63 ± 0.07(−12)	6.34(−12)	7.52(−12)

[a] Reference 19. [b] Reference 82.

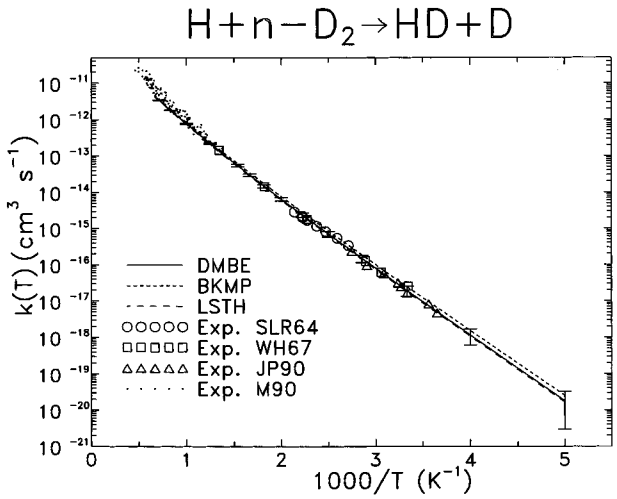

Figure 5. Arrhenius plot of the QCT thermal rate constants *k(T)* for the H + *n*-D_2 → HD + D reaction calculated on the three *ab initio* PESs, LSTH, DMBE, and BKMP, represented with lines as indicated. The symbols represent experimental results as follows: ref 81 (circles); ref 3 (squares); ref 83 (triangles); ref 82 (dots).

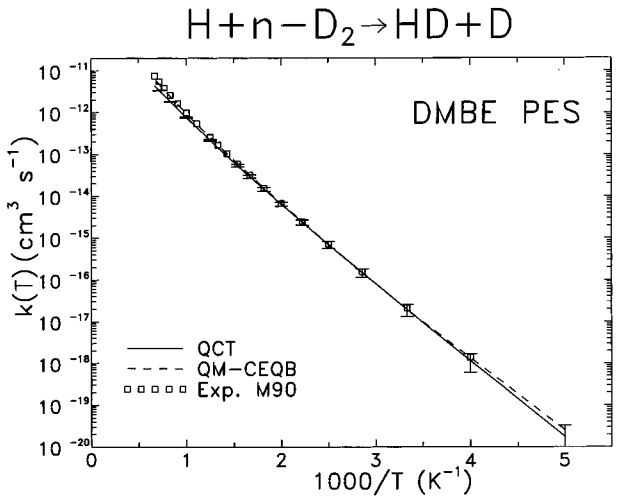

Figure 6. Arrhenius plot of the QCT thermal rate constants *k(T)* for the H + *n*-D_2 → HD + D reaction calculated on the DMBE PES (solid line). The QM-CEQB results of ref 19 (dashed line) and the three-parameter Arrhenius-like fit to the experimental data as given in ref 82 (squares) are also represented.

energy of the deuterium and hydrogen molecules. Furthermore, the conventional TST yields a ratio of pre-exponential factors, which, in this case, is nearly 1 and changes very little with temperature. On the other hand, the three parameter (A, n, E') empirical formula $k(T) = AT^n \exp(E'/k_BT)$ used by Michael[82] to fit most of the available experimental data gives values of the quotient of pre-exponential factors that range from 0.7 at 300 K to 0.95 at 1500 K, whereas the ratio of exponential factors reflects again the difference of zero-point energies (0.08 eV). Notice that, in both cases, the energy parameter appearing in the exponential factor is independent of temperature. Similar results were already obtained by Westenberg and Haas[3] from a two-parameter Arrhenius fit to the measured rate constants in the 450−750 K temperatute range. They concluded that the ratio of pre-exponential factors would be given by the ratio of collision frequencies *assuming the same collision cross sections for the two isotopic variants.*[3]

However, it has been shown in the previous section that the D + H_2/H + D_2 reaction cross section ratio at a given collision energy is notably larger than 1. Given this fact, an important question to address is how this ratio of cross sections shows up in the kinetic isotope effect. In order to uncouple approximately the respective contributions of threshold and cross section (reactive size) to the rate constant, it is convenient to use an empirical formula for the energy dependent reaction cross section in order to obtain an analytical rate constant expression via eq 10. A functionality of the type[96]

$$\sigma_R(E_T) = C\frac{(E_T - E_0)^n}{E_T}\exp[-m(E_T - E_0)] \qquad (12)$$

which can be related to the modified line of the centers model,[97,98] is flexible enough to fit the calculated QCT excitation functions. In this expression, C, n, m, and E_0 are adjustable parameters obtainable from the least-squares fit to the quasi-classical $\sigma_R(E_T)$. The resulting values of n and m are very similar for the two isotopic variants, whereas the values of C and E_0 are significantly different. By introducing this $\sigma_R(E_T)$ dependence in eq 10, one gets

$$k(T) = \frac{2^{3/2}C(k_BT)^{n-1.5}\Gamma(n+1)}{(\pi\mu)^{1/2}(mk_BT+1)^{n+1}}\exp(-E_0/k_BT) \qquad (13)$$

where the dependence of the rate constant on the absolute value of the cross section, essentially given by C, is solely contained

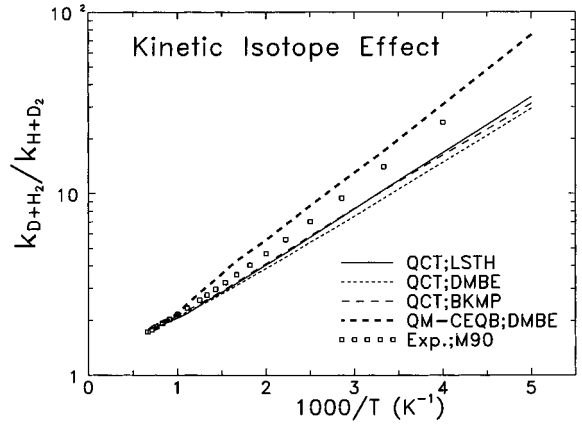

Figure 7. Ratio of the rate constants for the D + *n*-H_2 → HD + H and H + *n*-D_2 → HD + D reactions as a function of the temperature (kinetic isotope effect). Solid line: QCT calculation on the LSTH PES. Short dashed line: QCT calculation on the DMBE PES. Dashed line: QCT calculation on the BKMP PES. Thick dashed line: quantum mechanical calculation from ref 19. Squares: experimental data from the three-parameter Arrhenius-like fit of ref 82.

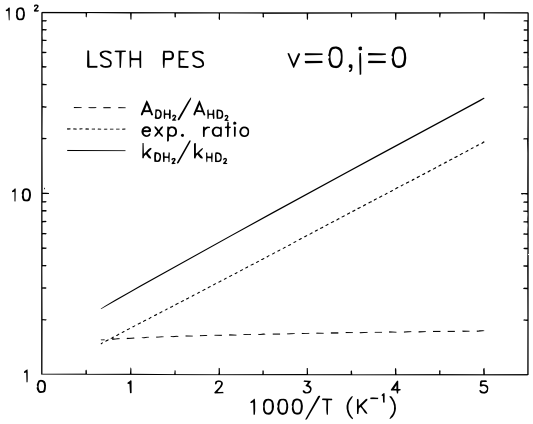

Figure 8. Kinetic isotope effect for the D + H_2 and H + D_2 reactions for $v = 0$, $j = 0$ on the LSTH PES calculated via eqs 12 and 13 (see text for more details). The solid line represents the ratio of rate constants. The long dashed and short dashed lines represent the ratio of pre-exponential (denoted as A) and exponential factors, respectively.

in the pre-exponential factor, and the dependence on the threshold, E_0, in the exponential one. By using eq 13, we can estimate the distinct contributions of threshold and cross section to the kinetic isotope effect. Figure 8 shows the quotient of exponential and pre-exponential factors from eq 13 for the D + H_2(v=0,j=0)/H + D_2(v=0,j=0) rate constant ratio. As can be seen, the quotient of exponential factors exhibits a sharp decrease with growing temperature and in the limit of infinite temperature tends to 1. However, the quotient of pre-exponential factors is only slightly dependent on temperature and is about 1.6, essentially given by the ratio between the $C/\mu^{1/2}$ factors for the two isotopomers. This result is at variance with the one obtained from conventional TST or the empirical three-parameter formula. At low temperatures, the influence of the different threshold for D + H_2 and H + D_2 is preponderant in the rate constant ratio; for temperatures of about 500 K the quotient of pre-exponential factors accounts for about one-third of the rate constant ratio, and at 1500 K both factors become comparable. Whereas the behavior of the ratio of exponential factors is a natural consequence of the threshold location and the Boltzmann distribution of collision energies, the dynamical origin of the smaller reaction cross section of H + D_2(v=0,j=0) as compared with D + H_2(v=0,j=0) is not so obvious.

The next step is to see if an indication of the larger reactive

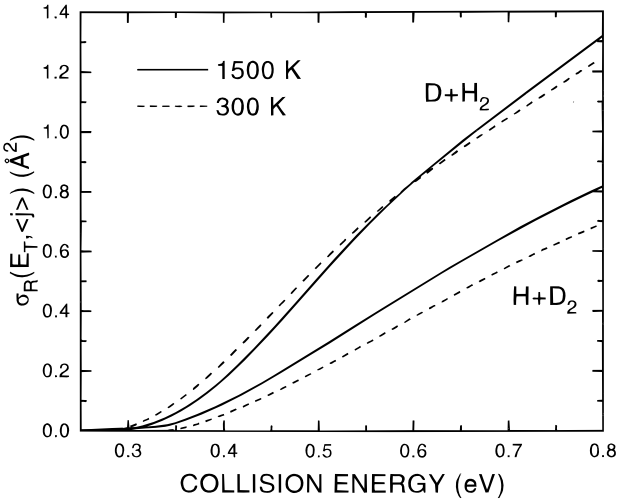

Figure 9. QCT excitation functions for the D + H_2 and H + D_2 reactions averaged on initial j for 300 and 1500 K calculated on the LSTH PES.

size of the D + H_2 reaction in comparison with H + D_2 can be found in the ratio of pre-exponential factors obtained from rate constants, thermally averaged on initial j. In this case, the threshold of the *effective* reaction cross section averaged on j will depend on T, since the reaction threshold for both isotopic variants changes with initial j, and the statistical weight of each j changes with temperature. This is clearly shown in Figure 9, where the change in the threshold and in the values of the cross section at 300 and 1500 K for the two reactions is apparent. Due to the opposite effect of rotation for the two isotopic variants, the excitation functions are closer to each other for thermally averaged j than for $j = 0$ (see Figures 1−3), and what is more important, the thresholds tend to the same value as the temperature increases. Therefore, for thermally averaged j results, eq 13 is only applicable for a given T, since now C, n, m, and very especially E_0, are temperature dependent. From the excitation functions shown in Figure 9 and by application of eqs 12 and 13, a quotient of D + H_2/H + D_2 pre-exponential factors of about 1.4, reflecting approximately the cross section ratio, is found for both temperatures. This result cannot be accounted for by conventional TST nor by the three-parameter Arrhenius-like formula, which assume a T independent energy parameter in the exponential factor. As a consequence, the ratio of pre-exponential factors obtained with these treatments does not provide any hint about the relative reactive sizes.

In spite of the fact that the difference in the absolute value of the reaction cross section is not clearly reflected in the KIE, it is evident that the D + H_2 reaction cross section is larger than that of the H + D_2, and as mentioned before, a similar effect has been experimentally observed in the corresponding reactions with D^- and H^-.[87] The origin of the different value of reaction cross sections and of their distinct dependence on rotation for the two isotopic variants under study remain to be explained. If the higher threshold energy of H + D_2 due to a lower zero-point energy were the only cause for the difference of reaction cross sections, one would expect the excitation functions for the two isotopomers to be represented by approximately parallel curves just shifted by the threshold energy difference. Such a behavior has been found, for instance, for the Cl + H_2(D_2) system, where the cross sections become almost identical when represented as a function of the total energy,[43] revealing very similar dynamics for the two isotopic variants. This is, however, not the case for the reactions under study, as clearly shown in Figure 10, where the cross sections of the two isotopic variants are plotted for $j = 0$ and $j = 3$, both as a

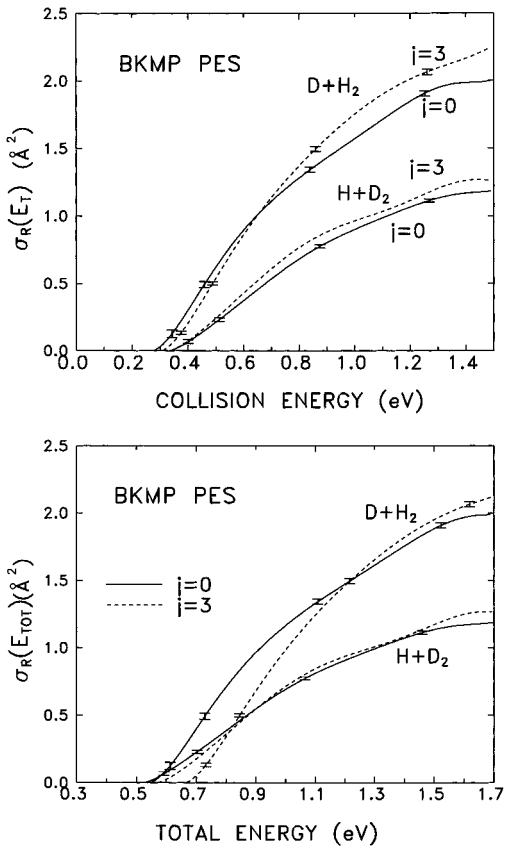

Figure 10. Top panel: QCT excitation functions calculated on the BKMP PES for the two isotopic variants of the hydrogen exchange reaction D + H_2 and H + D_2 for initial $v = 0$ and $j = 0$, 3. Bottom panel: same as the top panel but as a function of the total energy.

function of collision energy and as a function of total energy. The difference between the two thresholds for reaction with rotationless molecules coincides approximately with the difference in the zero-point energies of D_2 and H_2, and in fact, when plotted as a function of total energy, the two reactions have practically the same threshold. However, after the threshold the reaction cross section for H + D_2 grows slower with collision energy than that of D + H_2. Once more, the difference in the reagents' zero-point energy cannot explain the different reactivity.

Let us consider first the differences in the excitation functions with rotational excitation. The potential energy surface of the H_3 system is strongly collinear, and for this type of surface, and low collision energies, molecular rotation is expected to perturb the atom−diatom orientations favorable for reaction. This disorienting influence of rotation is more obvious in the cross section dependence on total energy, rather than on collision energy. In this representation, rotation is seen to cause a decrease in reactivity in the post-threshold region for both isotopic variants. The effect is comparatively slight in the H + D_2 case and is superseded in the translational excitation function by the increase in the available energy associated with the rotational excitation. For D + H_2, the disorienting effect of rotation is much more pronounced and prevails in $\sigma_R(E_T)$ up to collision energies of ∼0.7 eV.

In general, the disorienting effects of rotation are expected to be of importance in the post-threshold region, where the steric hindrances imposed by the potential are more severe and the reacting geometries of the three nuclei are limited to a more or less narrow "cone of acceptance". Unless the radial velocity of the reagents is high enough as compared with the angular velocity of the rotating molecule, the colliding partners might fail to pass through the cone of acceptance. This negative effect will be more marked for quick rotation and slow collision velocity. In simple terms, and neglecting the orbital relative motion, the decrease of the distance between the atom and the center of mass of the molecule, ΔR, during the time in which the molecule rotates by $\Delta\gamma$ (where $\Delta\gamma$ is the variation in the angle formed by R and the internuclear axis of the diatom), at a given collision energy, E_T, and initial rotational number, j, is given by[43]

$$\left(\frac{\Delta R}{\Delta\gamma}\right)^2 = \frac{I_{BC}E_T}{\mu_{A,BC}E_{rot}} = \frac{2E_T r_e^4 \mu_{BC}^2}{j(j+1)\hbar^2\mu_{A,BC}} \qquad (14)$$

where I_{BC} is the moment of inertia of the diatom, μ_i are the reduced masses, and $E_{rot} = j(j + 1)\hbar^2/2I_{BC}$ is the rotational energy.

The comparison of $\Delta R/\Delta\gamma$ for the two isotopic variants of the reaction yields[43]

$$\left(\frac{\Delta R}{\Delta\gamma}\right)_{DH_2} = \frac{\mu_{H_2}}{\mu_{D_2}}\left(\frac{\mu_{H,D_2}}{\mu_{D,H_2}}\right)^{1/2}\left(\frac{\Delta R}{\Delta\gamma}\right)_{HD_2} \qquad (15)$$

The quotient of reduced masses is ∼0.45, implying that the disorienting effects of rotation will be more important for the D + H_2 reaction in accordance with the results of the QCT calculation. Incidentally, $(\Delta R)/\Delta\gamma)_{HH_2} = 0.55(\Delta R/\Delta\gamma)_{HD_2}$, in accordance with the intermediate effect of rotation on reactivity (negative, but very slight) obtained for the H + H_2 reaction[25,27] on the LSTH PES. Whereas the relative "kinematic sensitivity" to disorientation of the two isotopic variants is contained in eq 15, the actual magnitude of the dynamical disorientation will depend on the features of the PES. For the present system, the three *ab initio* surfaces considered produce similar effects, although somewhat more marked for the DMBE one, as discussed at length in our previous work.[7]

For the system under study, it has been often stated that the potential surface tends to steer the reactants into a collinear configuration and exerts thus a beneficial orienting influence on reactivity, which should be more evident in the absence of the perturbing effects of rotation. We will thus consider rotationless molecules in order to examine whether a distinct orienting effect of the surface can be the cause of the difference in the reaction cross sections for the isotopic variants under study. It has been suggested in the literature[75] that the orienting effect will be different depending on the velocity of approach, which for a fixed collision energy will depend only on the reduced mass of the reactants. A simple way to investigate the importance of this effect on the reactivity is to perform QCT calculations for different pairs of reaction partners with the same or different collision-reduced masses. The calculated excitation functions are displayed in the upper panel of Figure 11. In order to make the results strictly comparable, the calculations have been performed without zero-point energy in the reacting molecules. A fictitious hydrogen isotope X with a mass of 4/3 amu has been introduced for the comparison, so that X + D_2 has the same reduced mass, $\mu_{A,BC}$, as D + H_2, and X + H_2 the same as H + D_2. An inspection of this figure shows that, in spite of having the same reduced mass, the D + H_2 system is clearly more reactive than the X + D_2 one and, analogously, the cross section for X + H_2 is always larger than that of H + D_2. The apparent rule is that the heavier the attacking atom and the lighter the diatom, the larger the cross section. In view of these results, other causes, different from a velocity dependent

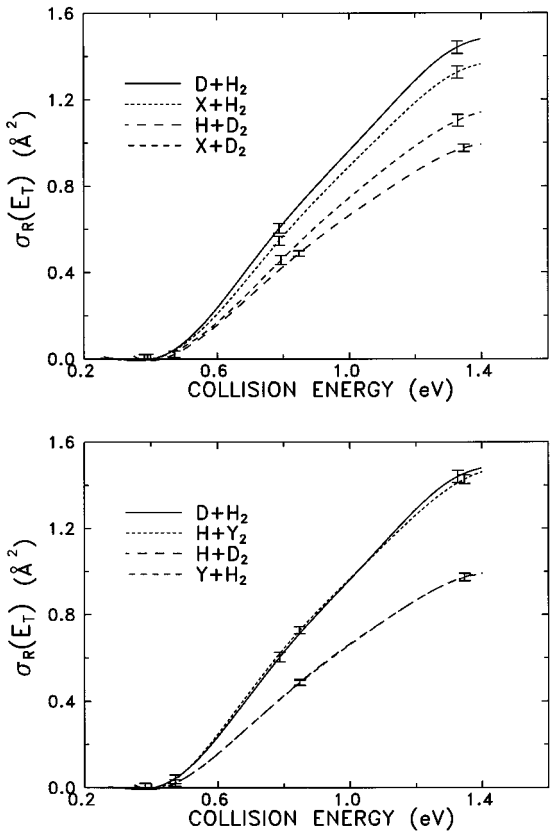

Figure 11. Excitation functions for a series of isotopic variants of the H_3 reaction calculated on the BKMP PES. In all cases the calculations have been carried out without zero-point energy and with rotationless molecules. Upper panel: the X fictitious isotope of mass 4/3 amu is chosen such that the relative reduced mass ($\mu_{A,BC}$) of the D + H_2 is the same as the X + D_2, whereas that of the H + D_2 is identical to that of X + H_2 reaction. Lower panel: the excitation function of the D + H_2 reaction is compared to that of the H + Y_2, and that of the H + D_2 is compared with that of the Y + H_2 reaction. Y is a fictitious isotope of mass 1/2, chosen in such a way that the "mass factors", F_b (see eq 16), are the same for each pair of reactions. As can be seen, the cross sections for reactions with the same F_b factor are practically identical.

orienting effect, must be sought for the distinct microscopic reactivity of the various isotopic variants.

The start of a reactive collision can be visualized in simple terms as a transfer of energy from the attacking atom to the molecular bond, which will thus be elongated and approach the saddle point configuration. For A + BC collisions in the "sudden limit", the transfer of collision energy to the BC bond, F_b, can be estimated by means of a well-known impulsive spectator model:[99,100]

$$F_b = \frac{\Delta E_b}{E_T} = \frac{4 m_A m_B m_C M}{m_{AB}^2 m_{BC}^2} \qquad (16)$$

where the ΔE_b is the fraction of the initial translational energy that can be transferred to the BC bond, the m_i represent the masses of the different atomic and molecular species involved, and M is the total mass of the system. Notice that this result is only dependent on a combination of masses and that systems with the same $F_b(=\sin^2 2\beta)$ have the same skew angle,[100] β, and, therefore, the same mass-scaled coordinates. If the likelihood of transfer of collision energy to the molecular bond as expressed by the mass quotient of eq 16 were the determinant factor for the reactivities of the different isotopic variants, one could expect very similar cross sections for reactions with isotope combinations yielding the same F_b, irrespective of their reduced masses. In order to verify this hypothesis, we will consider again rotationless molecules without zero-point energy like those of the previous paragraph and will introduce a fictitious isotope Y with a mass of 1/2 amu so that F_b for D + H_2 is the same as that of H + Y_2 and F_b for H + D_2 is the same as Y + H_2. The QCT excitation functions for these two pairs of isotopic variants are represented in the lower panel of Figure 11. As can be seen, the cross sections for pairs of isotopomers with the same F_b are identical over the whole energy range considered. The main consequence of this calculation is that, in fact, the key feature controlling the reactivity is the effectiveness of the transfer of collision energy to the diatomic bond. Furthermore, the excitation functions of any pair of isotopomers of H_3 can be scaled very approximately with the quotient of their respective F_b factors, as long as they have the same zero-point energy. The positive orienting influence of the surface on the reactivity, often invoked in the literature, is not clear from the results shown in Figure 11. In any case, although some indications have been found of a positive orienting influence of the surface that might enhance the reactivity, as shown in calculations carried out on different PESs for this reaction,[7] this effect is expected to be important only at low E_T and certainly cannot explain the difference in the cross sections over the whole range of collision energies investigated.

IV. Summary and Conclusions

Reaction cross sections and rate constants for the H + D_2 system have been obtained from quasiclassical trajectory calculations on three *ab initio* potential energy surfaces. The calculated thermal rate constants are in very good quantitative agreement with experiment and with the results of approximate quantum mechanical calculations in the temperature range between 250 and 800−900 K. At temperatures higher than 1000 K, the calculated rate constants become gradually smaller than the measured ones. No accurate quantum mechanical thermal rate constants have been reported for this isotopic variant of the reaction. The high-temperature disagreement might suggest possible shortcomings of the classical method, like an excessive recrossing of reactive trajectories back to the valley of the reactants or an inaccuracy in the region of the potential surface relevant for the rate constants. This last point is however unlikely, since dynamical experiments sampling higher energy regions have been well accounted for with both quantum mechanical and quasiclassical trajectory calculations. The fact that all theoretical calculations of rate constants for this and for the D + H_2 isotopic variant are to a greater or lesser extent smaller than the experimental data at high temperatures suggests also that an experimental reinvestigation of this region might be worthwhile.

In a previous quasiclassical trajectory study on the D + H_2 reaction, the effect of rotation was seen to be negative in the post-threshold region and the rate constants were found to be smaller than the experimental ones for temperatures lower than 350 K. The results of the present work show that rotational excitation always increases the reactivity of the H + D_2 system, and it is interesting to observe that the low-temperature rate constants are in good agreement with experiment. This finding lends additional support to the indications of the mentioned work on D + H_2, suggesting that the failure to account for the low-temperature behavior is related to the fact that the negative effect of rotation is exaggerated by the classical treatment near the threshold. The different influence of rotational excitation for the two isotopic variants can be rationalized in terms of the distinct kinematic sensitivity to disorientation by rotation.

Unfortunately a detailed study from accurate quantum mechanical calculations of cross sections for individual rotational states of $H_2(v=0)$ and $D_2(v=0)$ is not available. The performance of such calculations would be most interesting in order to clarify the distinct effect of rotation and its influence on the experimental observables like the rate constants.

Various effects contribute to the difference in the thermal rate constants for the two isotopic variants (kinetic isotope effect) over the temperature range considered. The higher threshold of H + D_2 (due to the lower zero-point energy of D_2) is the main reason of the much larger rate constants of D + H_2 at low temperatures. At high temperatures (T > 1000 K) the contribution of the relative reaction cross sections to the rate constant ratio becomes important. The marked effects of rotation on the reactivity of the two isotopomers lead to an appreciable temperature dependence of the effective threshold for reaction and has a clear influence on the kinetic isotope effect. The present dynamical results do not warrant the usual assumption of a fixed energy parameter in the exponential term of simple kinetic treatments, and therefore the conclusions that can be drawn from the comparison of pre-exponential factors about the relative reactive size can be misleading.

Calculations carried out with different isotopic variants of the H_3 system strongly suggest that the cause for the larger reaction cross sections of D + H_2 as compared with H + D_2 is the more efficient transfer of collision energy from the heavier D atom to the molecular bond, and these results can be rationalized with a simple dynamical model based on intuitive considerations.

Acknowledgment. We are indebted to Mark Brouard for his careful reading of the manuscript and his most valuable comments and to S. Schlemmer for letting us know his experimental results prior to publication. This work was financed by the DGICYT of Spain under Project PB95-0918-C03. The Spanish-British exchange program 'Acciones Integradas' is also acknowledged.

References and Notes

(1) Laidler, K. J. *Chemical Kinetics*, 3rd ed.; Harper & Row: New York, 1987, and references therein.
(2) Farkas, A.; Farkas, L. *Proc. R. Soc. London. A* **1935**, *152*, 124, and references therein.
(3) Westenberg, A. A.; De Haas, N. *J Chem. Phys*. **1967**, *47*, 1393.
(4) Garrett, B. C.; Truhlar, D. G. *J. Chem. Phys.* **1980**, *63*, 3460.
(5) Auerbach, S. M.; Miller, W. H. *J. Chem. Phys*. **1994**, *100*, 1103.
(6) Mielke S. L.; Lynch, G. C.; Truhlar, D. G.; Schwenke, D. W. *J. Phys. Chem*. **1994**, *98*, 8000.
(7) Aoiz, F. J.; Bañares, L.; Díez-Rojo, T.; Herrero, V. J.; Saéz Rábanos, V. *J. Phys. Chem*. **1996,** *100*, 4071.
(8) Park, T. J.; Light, J. C. *J. Chem. Phys.* **1991**, *94*, 2946.
(9) (a) Liu, B. *J. Chem. Phys*. **1963**, *58*, 1925. (b) Siegbahn, P.; Liu, B. *J. Chem. Phys*. **1978**, *68*, 2457. (c) Truhlar, D. G.; Horowitz, C. J. *J. Chem. Phys*. **1978**, *68*, 2466; **1979**, *71*, 1514(E).
(10) Varandas, A. J. C.; Brown, F. B.; Mead, C. A.; Truhlar, D. G.; Garrett, B. C. *J. Chem. Phys.* **1987**, *86*, 6258.
(11) Boothroyd, A. I.; Keogh, W. J.; Martin, P. G.; Peterson, M. R. *J. Chem. Phys*. **1991**, *95*, 4343.
(12) Chang, J.; Brown, N. J. *Int. J. Quantum Chem. Symp*. **1993,** *27*, 567.
(13) Chang, J.; Brown, N. J. *Int. J. Quantum Chem.* **1994,** *51*, 53(E).
(14) Chang, J.; Brown, N. J. *J. Chem. Phys.* **1995,** *103*, 4097.
(15) Chang, J.; Brown, N. J. *J. Phys. Chem.* **1996**, *100*, 17740.
(16) Ridley, B. A.; Schulz, W. R.; Le Roy, D. J. *J. Chem. Phys*. **1966**, *44*, 3344.
(17) Mitchell, D. N.; Le Roy, D. J. *J. Chem. Phys*. **1963**, *58*, 3449, and references therein.
(18) Michael, J. V.; Fisher, J. R. *J. Phys. Chem*. **1990**, *94*, 3318.
(19) Michael, J. V.; Fisher, J. R.; Bowman, J. M.; Sun, Q. *Science* **1990**, *249*, 269.
(20) Takada, S.; Ohsaki, A.; Nakamura, H. *J. Chem. Phys*. **1992**, *96*, 339.
(21) Wang, D.; Bowman, J. M. *J. Phys. Chem*. **1994**, *98*, 7994.
(22) (a) Karplus, M.; Porter, R. N.; Sharma, R. D. *J. Chem. Phys.* **1965,** *43* 3259. (b) Porter, R. N.; Karplus, M. *J. Chem. Phys.* **1964**, *40*, 1105.
(23) Blackwell, B. A.; Polanyi, J. C.; Sloan, J. J. *Chem. Phys.* **1977,** *24*, 25.
(24) Tan, K. G.; Laidler, K. J. *J. Chem. Phys.* **1977,** *67*, 5883.
(25) Barg, G.-D.; Mayne, H. R.; Toennies, J. P. *J. Chem. Phys.* **1981,** *74*, 1017.
(26) Sathyamurthy, N. *Chem. Rev*. **1983**, *83*, 601.
(27) Boonenberg, C. A. Mayne. H. *Chem. Phys. Lett.* **1984,** *67*, 108.
(28) Loesch, H. J. *Chem. Phys*. **1986**, *104*, 213.
(29) Loesch, H. J. *Chem. Phys*. **1987**, *112*, 85.
(30) Sathyamurthy, N.; Toennies, J. P. *Chem. Phys. Lett.* **1988,** *143*, 323.
(31) Grote, W.; Hoffmeister, M.; Schleysing, R.; Zerhau-Dreihöfer, H.; Loesch, H. J. In *Selectivity in Chemical Reactions*; Whitehead, J. C., Ed.; Kluwer: Dordrecht, 1989.
(32) Mayne, H. R. *Chem. Phys. Lett.* **1986**, *130*, 249.
(33) Mayne, H. R.; Minick, S. *J. Phys. Chem*. **1987**, *91*, 1400.
(34) Harrison, J. A.; Mayne, H. R. *J. Chem. Phys*. **1988**, *88*, 7424.
(35) Harrison, J. A.; Isakson, L. J.; Mayne, H. R. *J. Chem. Phys*. **1989**, *91*, 6906.
(36) Harrison, J. A.; Mayne, H. R. *Chem. Phys. Lett*. **1989**, *158*, 356.
(37) Kornweitz, H.; Persky, A.; Levine, R. D. *Chem. Phys. Lett*. **1986**, *128*, 443.
(38) Kornweitz, H.; Persky, A.; Schechter, I.; Levine, R. D. *Chem. Phys. Lett*. **1990**, *169*, 489.
(39) Levine, R. D. *J. Phys. Chem*. **1990**, *94*, 8863.
(40) Kornweitz, H.; Persky, A.; Levine, R. D. *J. Phys. Chem*. **1991,** *95*, 1621.
(41) Song, J. B.; Gislason, E. A. *J. Chem. Phys*. **1995,** *103*, 8884.
(42) Song, J. B.; Gislason, E. A. *Chem. Phys*. **1996**, *202*, 1.
(43) Aoiz, F. J.; Bañares, L. *J. Phys. Chem.* **1996,** *46*, 18108.
(44) Aoiz, F. J.; Herrero, V. J.; Sáez Rábanos, V. *J. Chem. Phys.* **1991,** *94*, 7991.
(45) Zhao, M.; Truhlar, D. G.; Schwenke, D. W.; Kouri, D. J. *J. Phys. Chem.* **1990,** *94*, 7074.
(46) Tsukiyama, K.; Katz, B.; Bersohn, R. *J. Phys. Chem.* **1986,** *84*, 1034.
(47) Johnson, G. W.; Katz, B.; Tsukiyama, T.; Bersohn, R. *J. Phys. Chem.* **1987,** *86*, 5445.
(48) Gerlach-Meyer, U.; Kleinermans, K.; Linnebach, E.; Wolfrum, J. *J. Chem. Phys.* **1987,** *86*, 3047.
(49) Levene, H. B.; Phillips, D. L.; Nieh, J.-C.; Gerrity, D. P.; Valentini, J. J. *Chem. Phys. Lett.* **1988,** *143*, 317.
(50) Schnieder, L.; Seekamp-Rahn, K.; Liedeker, F.; Steuwe, H.; Welge K. H. *Faraday Discuss. Chem. Soc.* **1991,** *91*, 259.
(51) Kitsopoulos, T. N.; Buntine, M. A.; Baldwin, D. P.; Zare, R. N.; Chandler, D. W. *Science* **1993,** *260,* 1605.
(52) Shafer, N. E.; Xu, H.; Tuckett, R. P.; Springer, M.; Zare, R. N. *J. Phys. Chem*. **1994,** *98*, 3369.
(53) Aoiz, F. J.; Bañares, L.; D'Mello, M. J.; Herrero, V. J.; Sáez Rábanos, V.; Schnieder, L.; Wyatt, R. E. *J. Chem. Phys*. **1994,** *101*, 5781.
(54) Schnieder, L.; Seekamp-Rahn, K.; Borkowski, J.; Wrede, E.; Welge, K. H.; Aoiz, F. J.; Bañares, L.; D'Mello, M. J.; Herrero, V. J.; Sáez Rábanos, V.; Wyatt, R. E. *Science* **1995,** *269*, 207.
(55) Xu, X.; Shafer-Ray, N. E.; Merkt, F.; Hughes, D. J.; Springer, M.; Tuckett, R. P.; Zare, R. N. *J. Chem. Phys*. **1995,** *103*, 5157.
(56) Wrede, E.; Schnieder, L.; Welge, K. H.; Aoiz, F. J.; Bañares, L.; Herrero, V. J. *Chem. Phys. Lett*. **1997,** *265*, 129.
(57) Wrede, E.; Schnieder, L.; Welge, K. H.; Aoiz, F. J.; Bañares, L.; Herrero, V. J.; Martínez-Haya, B.; Sáez Rábanos, V. *J. Chem. Phys.*, in press.
(58) Schnieder, L.; Seekamp-Rahn, K.; Wrede, E.; Welge, K. H. *J. Chem. Phys.*, submitted for publication.
(59) Gerrity, D. F.; Valentini, J. *J. Chem. Phys.* **1983,** *79*, 5202; **1984,** *81*, 1298.
(60) Marinero, E. E.; Rettner, C. T.; Zare, R. N. *J. Chem. Phys.* **1984,** *80*, 4142.
(61) Rinnen, K.-D.; Kliner, D. A. V.; Zare, R. N. **1989,** *91*, 7514.
(62) Adelman, D. E.; Xu, H.; Zare, R. N. *Chem. Phys. Lett.* **1993,** *203*, 563.
(63) D'Mello, M.; Manolopoulos, D. E.; Wyatt, R. E. *J. Chem. Phys.* **1991,** *94*, 5985.
(64) Mielke, S. L.; Truhlar, D. G.; Schwenke, D. W. *J. Phys. Chem.* **1994,** *98*, 1053.
(65) D'Mello, M.; Manolopoulos, D. E.; Wyatt, R. E. *Science* **1994,** *263*, 102.
(66) Kuppermann, A.; Wu, Y.-S. M. *Chem. Phys. Lett.* **1995,** *241*, 229.
(67) Wu, Y.-S. M.; Kuppermann, A. *Chem. Phys. Lett.* **1995,** *235*, 105.
(68) Schatz, G. C. *Chem. Phys. Lett.* **1884,** *108*, 532.
(69) Connor, J. N. L.; Southall, W. J. E. *Chem. Phys. Lett.* **1984,** *108*, 527.
(70) Suck, S. H.; Klein, C. R.; Lutrus, C. K. *Chem. Phys. Lett.* **1984,** *110*, 112.

(71) Bowers, M. S.; Choi, B. H.; Poe, R. T.; Tang, K. T. *Chem. Phys. Lett.* **1985,** *116,* 239.
(72) Connor, J. N. L.; Southall, W. J. E. *Chem. Phys. Lett.* **1986,** *123,* 139.
(73) Last, I.; Ron, S.; Baer, M. *Isr. J. Chem.* **1989,** *29,* 451.
(74) Baram, A.; Last, I.; Baer, M. *Chem. Phys. Lett.* **1993,** *212,* 649.
(75) Mayne, H. R *J. Chem. Phys.* **1980,** *63,* 217.
(76) Blais, N. C.; Truhlar, D. G. *Chem. Phys. Lett.* **1983,** *102,* 120.
(77) Blais, N. C.; Truhlar, D. G. *J. Chem. Phys.* **1985,** *83,* 2201.
(78) Schechter, I.; Levine, R. D. *Int. J. Chem. Kinet.* **1986,** *18,* 1023.
(79) Blais, N. C.; Truhlar, D. G. *Chem. Phys. Lett.* **1989,** *162,* 503.
(80) Aoiz, F. J.; Bañares, L.; Herrero, V. J. *J. Chem. Phys.* **1996,** *105,* 6086
(81) Schulz, W. R.; LeRoy, D. J. *Can. J. Chem.* **1964,** *42,* 2480.
(82) Michael, J. *J. Chem. Phys.* **1990,** *92,* 3394.
(83) Jayaweera, I. S.; Pacey, P. D. *J. Phys. Chem.* **1990,** *94,* 3614.
(84) Sun, Q.; Bowman, *J. Phys Chem.* **1990,** *94,* 718.
(85) Zhang, J. Z. H.; Miller, W. H. *J. Chem. Phys.* **1989,** *91,* 1528.
(86) Aoiz, F. J.; Herrero, V. J.; Sáez Rábanos, V. *J. Chem. Phys.* **1992,** *97,* 7423.
(87) Schlemmer, S. Private communication.
(88) Song, J. B.; Gislason, E. A. *Chem. Phys*. **1997**, *214*, 23.
(89) Aoiz, F. J.; Bañares, L.; Herrero, V. J.; Stark, K.; Werner, H.-J. *Chem. Phys. Lett.* **1996**, *254*, 341.
(90) Aoiz, F. J.; Bañares, L.; Herrero, V. J.; Sáez Rábanos, V.; Stark, K.; Tanarro, I.; Werner, H.-J. *Chem. Phys. Lett.* **1996**, *262*, 175.
(91) Huber, K. P.; Herzberg G. *Molecular Spectra and Molecular Structure*. *Part IV. Constants of Diatomic Molecules;* Van Nostrand: New York, 1979.
(92) Dabrowski, I.; Herzberg, G. *Can. J. Phys.* **1976,** *54,* 525.
(93) Kolos, W.; Wolniewicz, L. *J. Mol. Struct.* **1975,** *54,* 303.
(94) Truhlar, D. G.; Muckerman, J. T. In *Atom-Molecule Collision Theory;* Bernstein, R. B., Ed.; Plenum: New York, 1979.
(95) Wrede, E.; Schnieder, L.; Welge, K. H.; Aoiz, F. J.; Bañares, L.; Herrero, V. J.; Martínez-Haya, B.; Sáez Rábanos, V. *J. Chem. Phys.* **1997**, *106*, 7862.
(96) Varandas, A. J. C. *Chem. Phys.* **1982,** *69,* 295.
(97) Levine, R. D.; Bernstein, R. D. *Chem. Phys. Lett.* **1984,** *105,* 467.
(98) Smith, I. W. M. *J. Chem. Ed.* **1982,** *9*, 59.
(99) Mahan, B. H. *J. Chem. Phys.* **1970,** *52,* 5221.
(100) Levine, R. D.; Bernstein, R. B. *Molecular Reaction Dynamics and Chemical Reactivity*; Oxford University Press: New York, 1987.